JOURNAL OF CATALYSIS 113, 466–474 (1988)

IR Investigation of CO Adsorbed on Co Particles Obtained via $Co_2(CO)_8$ Adsorbed on MgO and SiO_2

K. MOHANA RAO,[1] G. SPOTO, AND A. ZECCHINA[2]

Dipartimento di Chimica Inorganica, Chimica Fisica e Chimica dei Materiali, Università di Torino, Corso M. D'Azeglio 48, 10125 Torino, Italy

Received December 16, 1987; revised April 14, 1988

Gas-phase adsorption of $Co_2(CO)_8$ on totally dehydroxylated MgO occurs with the loss of CO and the formation of higher nuclearity clusters both neutral and negatively charged. Subsequent decarbonylation and reduction in hydrogen at 673 K produces finely divided cobalt particles. These particles on successive interaction with carbon monoxide ($p \leq 5 \times 10^{-1}$ Torr) give the expected IR manifestations of CO adsorbed on finely divided cobalt (i.e., the appearance of a peak shifting from 2040 cm^{-1} at p_{CO} = 40 Torr to 2007 cm^{-1} at $p_{CO} < 10^{-3}$ Torr). In addition to these features, other peaks appear at lower frequencies (particularly at $p_{CO} \geq 0.5$ Torr) which are due to $Co(CO)_4^-$ and CO_3^{2-}-like species adsorbed on the matrix. Parallel experiments carried out on the $Co_2(CO)_8/SiO_2$ system give only a single CO peak shifting from 2050 cm^{-1} (p_{CO} = 40 Torr) to 2015 cm^{-1} ($p_{CO} < 10^{-3}$ Torr) which is assigned to the stretching of CO on Co particles supported on SiO_2. The comparison of the two sets of results indicates that, on the Co/MgO system, the metallic particles lose cobalt atoms in the form of $Co(CO)_4^-$ entities (which are stabilized on the basic ionic matrix) but that this effect is missing when the supporting oxide is SiO_2. This new type of metal–support interaction is discussed in terms of a nucleophilic attack of the highly basic O^{2-} ions of the MgO surface on the Co–CO groups located at the border of the metallic particles. The analogy with the homogeneous reactions of cobalt carbonyls in basic media is also discussed.

INTRODUCTION

The valency state of metals supported on the surface of oxides depends upon many factors, e.g., the impregnation technique, the reducing agent, and the time and temperature of the reducing procedure.

In many cases, even when noble metals are used, evidence has been produced for the presence of unreduced or incompletely reduced metal cations, even after many hours of reduction (*1*). A way to overcome the uncertainty associated with the impregnation techniques is to dose the metal directly from the vapor phase onto the support. This is the case with the Mg/MgO system recently studied in our laboratory (*2*). Unfortunately this method can be used only with metals with low melting points and does not have wide applicability. Metal atoms can be easily dosed on oxide single crystals by means of atomic beams (*3*), but this method cannot be applied to obtain dispersed metals on high-surface-area powders. However, metals in the zero-valent state can be transported onto high-surface-area supports as volatile metal carbonyls from the gas phase by the method of sublimation under vacuum. Provided that the surface is rigorously free of OH groups and of adsorbed water, the complex can in principle remain in the zero-valent state. This is indeed the case for the interaction of $Co_2(CO)_8$ with the surface of highly dehydroxylated silica, where, at 300 K, only a moderate decarbonylation leading to $Co_4(CO)_{12}$ and possibly higher nuclearity clusters is observed (*4, 5*).

The situation is slightly different when the interaction of $Co_2(CO)_8$ with fully dehydroxylated MgO is considered. In fact, in addition to the presence of adsorbed $Co_2(CO)_8$, $Co_4(CO)_{12}$, and higher nuclearity

[1] On leave from Indian Institute of Technology, Bombay, India.

[2] To whom correspondence should be addressed.

0021-9517/88 $3.00

clusters (derived from a similar decarbonylation process), considerable amounts of CO_3^{2-} and negatively charged carbonylic species are also formed when $Co_2(CO)_8$ is dosed under vacuum (*4*). Moreover, in the presence of CO gas, a disproportionation reaction also occurs, which, without altering the mean zero oxidation state of cobalt, leads to the formation of equivalent amounts of $Co^{2+}(CO)_n$ and $Co(CO)_4^-$ species.

Fortunately this last reaction is not predominant in the absence of a CO atmosphere: consequently we can conclude that the dosing of $Co_2(CO)_8$ from the gas phase onto the surface of totally dehydrated MgO represents a way of covering the surface with a zero-valent cobalt compound.

Once the carbonyl is safely transported onto the surface *in vacuo*, the metallic cobalt could, in principle, be obtained simply by decarbonylation *in vacuo*. However, the process of decarbonylation is not necessarily a simple one because disproportionation reactions and CO fragmentation can lead to the partial formation of carbidic and/or oxidic compounds. As a consequence, a reducing step involving hydrogen, which is capable of removing small amounts of carbon and oxygen, must always follow the decarbonylation procedure.

The procedure outlined above is not per se able to ensure that all the deposited cobalt is in the zero-valent state (as in the case of direct deposition from the gas phase); however, it is one of the most clean and less oxidizing chemical procedures that we can hypothesize.

In this paper we examine and compare the surface properties of cobalt obtained from gas-phase deposition of $Co_2(CO)_8$ on fully dehydroxylated MgO and highly dehydrated SiO_2. The surface properties are probed by using CO as a test molecule.

EXPERIMENTAL

High-surface area (~200 $m^2\ g^{-1}$) MgO pellets, suitable for IR investigations, have been prepared by decomposition of $Mg(OH)_2$ *in vacuo* at 523 K. The complete dehydroxylation of the surface has been achieved by outgassing the pellet *in vacuo* ($p < 10^{-5}$ Torr) at 1073 K for several hours (*4*).

The silica used was Aerosil Degussa (380 $m^2\ g^{-1}$) outgassed at 1123 K for a comparable time. Unlike in the MgO case, this procedure is not able to remove completely the surface hydroxyls (a residual concentration $n_{OH}/100\ Å^2 \approx 1.5$ is still remaining) (*6*). Higher outgassing temperatures must be avoided because they cause sintering of the sample. The IR spectra have been obtained on a Perkin–Elmer 580B instrument equipped with a data station. Pellets of MgO and SiO_2 containing 15–20 mg/cm^2 of powder and a low-path-length (0.7-cm) quartz IR cell were used in the experiments.

RESULTS AND DISCUSSION

1. *Adsorption of $Co_2(CO)_8$ on MgO and SiO_2*

Figure 1A shows the IR spectra obtained when $Co_2(CO)_8$ is dosed on MgO *in vacuo* through gas-phase sublimation. The different curves correspond to increasing doses of cobalt carbonyl on the MgO surface, the highest intensity spectrum corresponding to about 2% by weight cobalt loading.

A detailed description of these spectra and their assignments are reported elsewhere (*4*). We only mention here, briefly, that the overall spectrum can be explained in terms of $Co_2(CO)_{8_{ads}}$, $Co_4(CO)_{12_{ads}}$ and $Co_m(CO)_{n_{ads}}$ zero-valent clusters (deriving from adsorbed $Co_2(CO)_8$ by the loss of CO in the gas phase) and of $Co(CO)_4^-$, $Co_m(CO)_n^-$, and CO_3^{2-} species formed via a complex sequence of reactions initiated by the nucleophilic attack of surface O_{cus}^{2-} (cus: coordinatively unsaturated) ions on the CO ligands of adsorbed zero-valent clusters.

Figure 1B shows the IR spectra of increasing amounts of $Co_2(CO)_8$ on SiO_2 obtained by dosing under vacuum through gas-phase sublimation. Also, in this case

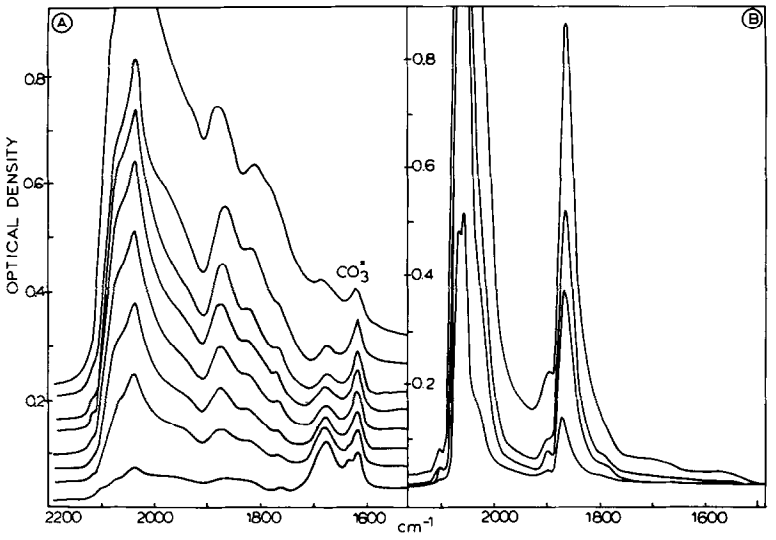

FIG. 1. (A) IR spectra of increasing doses of $Co_2(CO)_8$ adsorbed through gas phase sublimation on MgO. (B) IR spectrum of increasing doses of $Co_2(CO)_8$ adsorbed through gas-phase sublimation on SiO_2.

the maximum coverage corresponds to about 2% by weight cobalt loading. A detailed discussion has been given elsewhere (*4*). It is sufficient to mention here that the spectra can be interpreted only in terms of the predominant presence of adsorbed $Co_4(CO)_{12}$, without formation (as in the case of MgO) of negatively charged clusters.

2. *CO Adsorption on Co/MgO*

After adsorption of $Co_2(CO)_8$ on fully dehydrated MgO (last dose of Fig. 1A), the sample has been decarbonylated and reduced *in vacuo* at 673 K. The IR spectrum of the resulting black sample does not show traces of residual carbonylic compounds. The effect of dosing CO at two different pressures (0.4 and 40 Torr) is illustrated in Fig. 2.

The following comments can be made:

(a) at the lowest pressure (0.4 Torr) peaks are observed at 2025, 1940, 1880, 1855, 1665, 1610, 1520, 1370, 1320, and 1285 cm^{-1} (the peak at 2025 cm^{-1} represents the strongest feature of the spectrum);

(b) by increasing the pressure from 0.4 to 40 Torr, the peak at 2025 cm^{-1} undergoes an upward shift to 2040 cm^{-1} (accompanied by some broadening and an intensity decrease); and

(c) by increasing the pressure from 0.4 to 40 Torr CO, the triplets at 1940, 1880, and 1855 cm^{-1} and the other low-frequency bands undergo strong intensification.

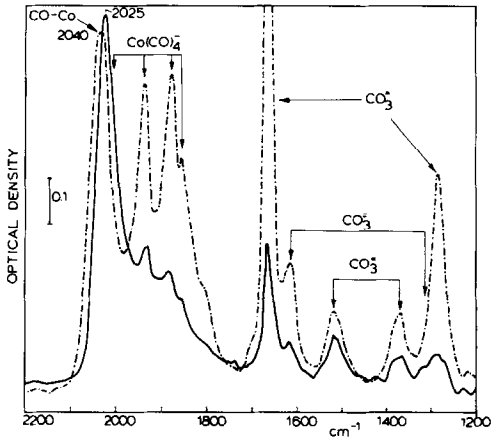

FIG. 2. IR spectrum of CO adsorbed on cobalt particles obtained from decarbonylation at 673 K of $Co_2(CO)_8$ adsorbed on MgO and successive reduction in H_2 at the same temperature. Solid line, 0.4 Torr CO; dotted line, 40 Torr CO.

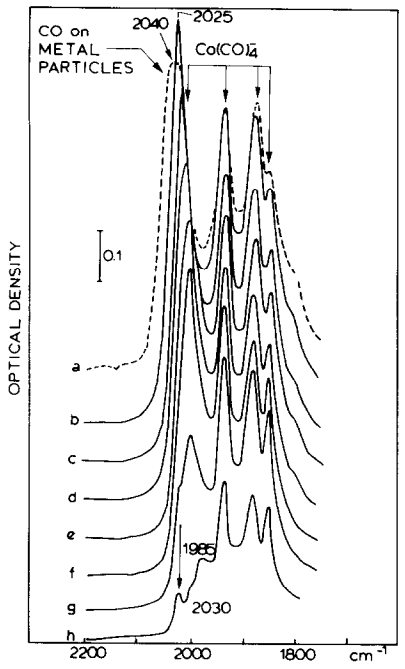

FIG. 3. CO desorption at room temperature and at increasing temperatures from the Co/MgO system. (a) 40 Torr of CO on metal particles; (b, c, d, e, and f) are obtained when (a) is evacuated for 10 s, 70 s, 5 min, 30 min, and 60 min, respectively. (g and h) are obtained by evacuating at 10^{-3} Torr for 5 min at 373 and 423 K, respectively.

As schematically indicated in Fig. 2, we assign the peak at 2025–2040 cm^{-1} to the stretching mode of CO adsorbed on cobalt microparticles. This assignment is based on (I) comparison with the literature data (*7, 8*), and (II) the unique behavior of this band upon a CO pressure increase (undoubtedly associated with compression effects) (*9*).

This assignment is further confirmed by the experiments illustrated in Fig. 3 (vide infra). The peaks of the triplet at 1940, 1880, and 1855 cm^{-1} grow in a parallel way, without change in frequency and relative intensity, when adsorption (Fig. 2) and desorption (Fig. 3) experiments are conducted. These facts together with the small half-width of the single peaks suggest that a single well-defined species is involved. The triplet is assigned to a distorted form of $Co(CO)_4^-$ adsorbed on MgO. This is based on:

(I) comparison with the literature data (*10*) concerning $Co(CO)_4^-$ in different solvents and in the presence of different counter ions;

(II) the spectra of $Co(CO)_4^-$ on MgO (*11*) as formed by reduction of a dilute CoO–MgO solid solution in CO (an assignment given also on the basis of ^{12}CO–^{13}CO isotopic substitution experiments); and

(III) the spectrum of $Co(CO)_4^-$ on MgO (*4*) as formed from adsorbed $Co_2(CO)_8$ by interaction with Lewis bases (NH_3) or in the presence of a high CO pressure (*4*). The fourth mode in this species, expected at 2030 cm^{-1} (*10, 11*), is obscured by the high-intensity band of CO on cobalt particles and is revealed only during the desorption experiment (Fig. 3; vide infra).

The assignment of the 2030, 1940, 1880, and 1855 cm^{-1} quartet to a low-symmetry $Co(CO)_4^-$ species is also proved by the following considerations. The free $Co(CO)_4^-$ is tetrahedral and belongs to the T_d group. Hence the vibrational representation of the CO stretching modes is

$$\Gamma_{CO} = A_1 + T_2,$$

where A_1 is Raman active and, T_2 is IR active (triply degenerate).

In the solution of a highly solvating solvent, these modes are located at 2010 and 1895 cm^{-1} (*12*). If k and i are the force and interaction constants, then the two frequencies are given by the equations

$$K = k + 3i \quad (A_1)$$
$$K = k - \ i \quad (T_2).$$

As the $Co(CO)_4^-$ with T_d symmetry has only one IR peak, the quartet in the 2030–1855 cm^{-1} range cannot be explained on this basis. If the $Co(CO)_4^-$ is distorted by an axial field or forms an adduct of the type shown in Scheme I, where the asterisk indicates a positive center, the symmetry changes from T_d *to* C_{3v}. The new vibrational representation is

$$\Gamma_{CO} = 2A_1 + E,$$

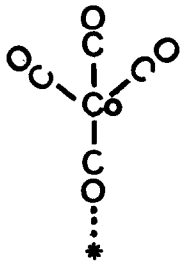

SCHEME I

where A_1 is IR active and E is doubly degenerate, IR active and three IR bands are expected in the IR spectrum. Following Brateman (*12*), the original T_2 mode splits into A_1 and E modes with frequencies

$$K = k - i + 2\delta$$

and

$$K = k - i - \delta,$$

where δ is the "distortion" parameter which represents the deviation from the T_d symmetry. It is evident that this structure also cannot explain the four bands observed in the spectrum. If a deeper distortion is introduced, then the original T_d symmetry can be lowered to C_{2v}. The $Co(CO)_4^-$ species can be now represented as shown in Scheme II where δ is the distortion parameter and the vibrational representation is

$$\Gamma_{CO} = 2A_1 + B_1 + B_2,$$

where the A_1, B_1, B_2 modes are all IR active. The frequencies of the four modes are now given by the equations

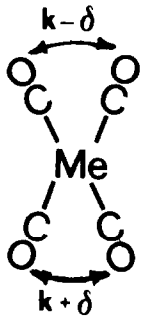

SCHEME II

$$\begin{vmatrix} (k - i + \delta) - K & 2i \\ 2i & k + i - \delta - K \end{vmatrix} \quad A_1$$

$$K = k - i + \delta \qquad B_1$$

$$K = k - i + \delta, \qquad B_2$$

(1)

where k and i ($\gg\delta$) are the same as those with the undistorted anion (and are available from the literature) (*12*).

In our case we are dealing with four bands. Thus, if $Co(CO)_4^-$ is present, it should be in C_{2v} local symmetry.

The k and i values can be considered, to a first approximation, an intrinsic property of the $Co(CO)_4^-$ anion. Consequently, the four frequencies can be approximated by using a single adjustable parameter only (δ). If all the data concerning $Co(CO)_4^-$ on MgO (*4*, *11*) are collected together in a single diagram where the frequency K is reported as a function of δ, Fig. 4 is obtained. This diagram is self-explanatory and greatly supports our assignment (especially because k

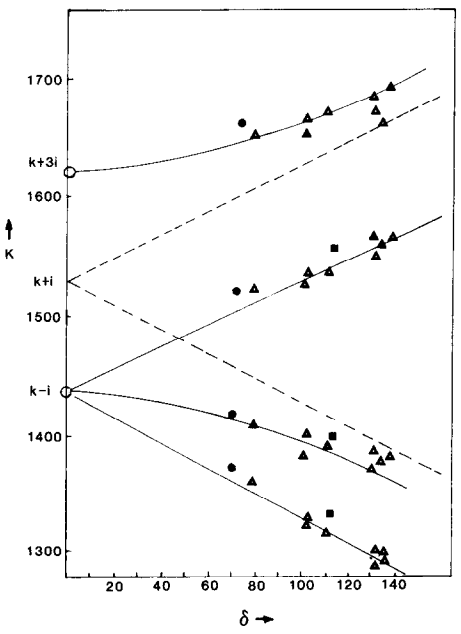

FIG. 4. K vs δ (in N m^{-1} units) ($K = 4.0383 \times 10^{-4}$ cm^{-2}). Solid lines ($i \gg \delta$) from Eq. (1) using k and i values from the literature (*12*); dashed lines refer to the limiting case where $\delta \gg i$. (●) Data from this experiment; (■) data from Ref (*4*); (△) data from Ref (*11*).

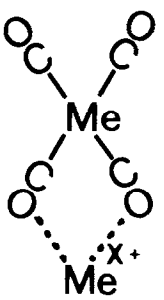

SCHEME III

and *i* coming from independent sources are used together with a single adjustable parameter).

Similar splitting effects are well known in solutions of $Co(CO)_4^-$ salts and are caused by the interaction of $Co(CO)_4^-$ with the counter-cation (*12, 13*). For instance, when highly solvating molecules are used as solvent, the cation–anion pair is solvent-separated and T_d symmetry is well approximated. When the solvation is absent or weak, the anion and the cation form a tightly bonded pair which causes distortion from T_d to C_{2v} symmetry as represented in Scheme III.

This is what is happening on the MgO surface, although in this case the $Co(CO)_4^-$ is under the simultaneous influence of more than one positive and negative center. For this reason, the distortion from T_d symmetry is influenced by the structure of the adsorbing sites: this explains why, depending upon the starting system (MgO–CoO solid solution (*11*), MgO–$Co_2(CO)_8$ (*4*), or, as in our case, Co^0–MgO), the quartet appears at differing frequencies (which are however all connected by the splitting diagram of Fig. 4).

The simple adduct of type *a* is not predominant here (unlike many other systems such as $Me(CO)_6$ and $Fe(CO)_5$ on γ-Al_2O_3, ZSM-5, and H–Y) (*14, 15*), because the Mg^{2+} ion is not a strong Lewis site.

It is most noticeable (results not described here for the sake of brevity, but fully discussed in other papers dealing with $Co(CO)_4^-$ on MgO) (*11*)) that successive dosing of NH_3 and or pyridine on preadsorbed CO causes a reversible modification of the $Co(CO)_4^-$ spectrum (the three low-frequency peaks coalesce into a single one at ~1880 cm^{-1}). This result is fully understandable only on the basis of the previous discussion. In fact, as the bases solvate the Mg^{2+} ions of the surface, the triplet of bands in the 1940–1855 cm^{-1} interval gradually merge into the very strong single peak (corresponding to the triply degenerate T_2 mode of a $Co(CO)_4^-$ species in T_d symmetry) because the tight $Co(CO)_4^-$–surface interaction is reduced by the formation of a monolayer of molecules coordinated on the Mg^{2+} ions.

A small presence of other negatively charged clusters like $Co_6(CO)_{11}^{4-}$, $Co_6(CO)_{14}^{4-}$ etc. (which have IR modes in the 2050–1600 cm^{-1} range) (16–18) cannot be excluded. However, we may recall that the high-nuclearity negatively charged cobalt carbonyl clusters have been found to disintegrate into mononuclear $Co(CO)_4^-$ anions in the presence of a sufficient pressure of CO (*4*).

Finally, the low-frequency peaks appearing in Fig. 2 (1665, 1610, 1520, 1370, 1320, and 1285 cm^{-1}) are assigned to a variety of surface carbonates (fundamentally of the bidentate type). This assignment is given on the basis of the comparison with the large amount of spectroscopic literature concerning surface carbonate-like species (*19*) and homogeneous compounds containing CO_3^{2-} species (*20, 21*).

It is worth mentioning that the $Co(CO)_4^-$ and carbonate species *appear with very similar speeds* in the same activated process.

We take the view that they originate during the same process, i.e., a nucleophilic attack of the O^{2-}_{ads} ions of the MgO surface on CO adsorbed on cobalt particles, following the scheme

$$2Co^0(CO) + 2O^{2-} \xrightarrow{CO} 2Co(CO)_4^- + CO_3^{2-}$$

which can be represented as in Scheme IV.

This process is similar to that already

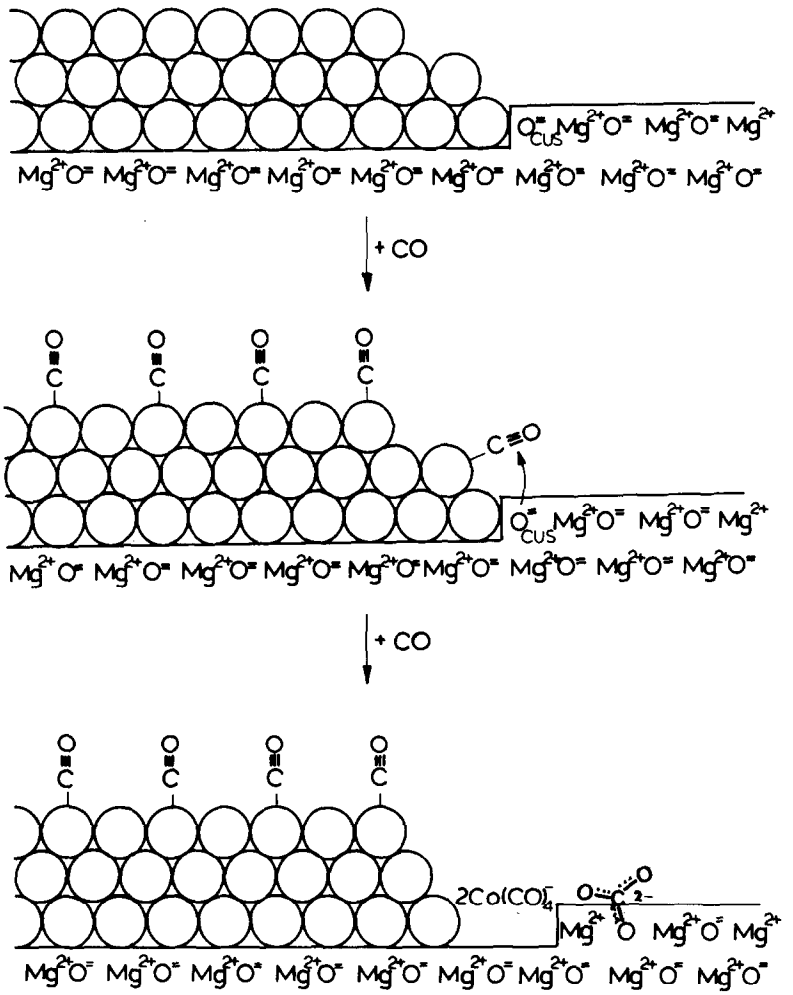

SCHEME IV. The cobalt particle is nucleated near the step or the corner position of MgO, characterized by a very coordinatively unsaturated oxygen ion (O^{2-}_{cus}), which, being capable of attacking the CO coordinated to a cobalt atom of the periphery of the particle, initiates sequence of reactions leading to $Co(CO)_4^-$ and CO_3^{2-}.

ascertained for the interaction of $Co_2(CO)_8$ with the MgO surface (*4*) and *represents a new type of CO activation via the simultaneous cooperation of the borderline metal atoms of the catalyst and the basic function* (O^{2-}) *of the support.*

Similar reaction between cobalt carbonyls and bases occur under homogeneous conditions (*22*).

It is most interesting that the activation of CO adsorbed on metals via the interaction with a Lewis acid site has already been postulated (Scheme II) (*23*). In Scheme V the interaction occurs via the O bonding of the terminal oxygen of CO with a Lewis acid site of the oxidic support.

In our opinion the present results represent the first clear observation of the participation of surface *basic* sites in CO activation. It is also noteworthy that the previous process represents an entirely new route leading to metal particle fragmentation and stabilization of the mononuclear fragments on the ionic support.

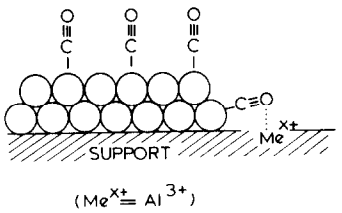

SCHEME V. The CO molecule coordinated at the periphery of the particle interacts with a Lewis acid center (in this case Al^{3+} of the Al_2O_3 support) via O bonding (*23*).

3. *CO Desorption from the Co/MgO System*

This experiment is illustrated in Fig. 3. The most relevant features are the following.

(a) Upon a decrease in the CO pressures to 10^{-3} Torr the 2040 cm^{-1} peak undergoes a downward shift to 2025 cm^{-1} with simultaneous narrowing and intensification. This effect has also been observed on other metals (*8, 9*) and has been interpreted in terms of a transition from out-of-registry to in-registry structures. Unfortunately no systematic observation on cobalt single crystals is actually known.

(b) By prolonged outgassing at room temperature a further intensity decrement is observed, accompanied by a further shift to lower frequencies. The nearly complete disappearance of the peak associated with CO adsorbed on metal particles is achieved at 423 K. At the lowest coverages the peak is observed at 1985 cm^{-1}. The 2040–1985 cm^{-1} shift is due to changes in the adsorbate–adsorbate (static and dynamic) interaction. The separation of the two contributions by means of the well-known ^{12}CO–^{13}CO isotopic substitution method (*9*) is outside the scope of this contribution.

(c) The peaks associated with the $Co(CO)_4^-$ entity are more resistant to the thermal treatment *in vacuo:* consequently once the main peak due to the CO adsorbed on cobalt particles has been eliminated, the expected low-intensity mode at 2030 cm^{-1} of the $Co(CO)_4^-$ is evidenced.

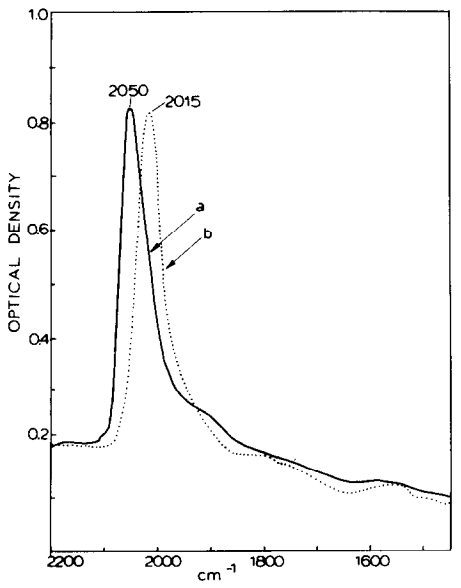

FIG. 5. CO adsorption and desorption on the Co/SiO_2 system (a) with 40 Torr CO, (b) after evacuation for 5 min at room temperature at 10^{-5} Torr.

4. *CO Adsorption on the Co/SiO_2 System*

This experiment has been made following the same procedure as that described for the Co/MgO system. After adsorption of $Co_2(CO)_8$ (corresponding to about 2% by weight of cobalt), the system has been decarbonylated *in vacuo* and reduced in hydrogen at 673 K. No sign of residual carbonylic groups could be detected after this treatment, indicating that the resulting cobalt particles are sufficiently clean.

Successive adsorption of CO (40 Torr) gives (Fig. 5) a single peak at 2050 cm^{-1} shifting to 2015 cm^{-1} by short evacuation at room temperature ($p < 10^{-3}$ Torr). By comparison with the previous experiment and with data from the literature (*7, 8*), this peak can be readily assigned to CO adsorbed on cobalt particles. The most important result of this experiment is represented by the total absence of the peaks due to CO_3^{2-} and $CO(CO)_4^-$.

This fact is not surprising because *the SiO_2 surface is very covalent and the nucleophilic groups, capable of interacting*

with the CO ligands, are totally absent. It is evident that this experiment totally confirms the previous conclusions concerning the Co/MgO system.

A further point deserving a separate comment is the lower value of the frequency of CO (p = 40 Torr) adsorbed on cobalt particles supported on MgO (2040 cm^{-1}) with respect to that on SiO_2 (2050 cm^{-1}). Whether this is due to a metal–support interaction (MgO acting as a donor surface) or due to the presence of different exposed faces is impossible to answer at this stage.

CONCLUSIONS

The interaction of CO with cobalt particles supported on MgO (fully dehydroxylated) and SiO_2 (highly dehydrated) gives different results. On the Co/MgO system, in addition to the IR peak of CO linearly adsorbed on Co^0, evidence is obtained for the nucleophilic attack of basic surface O^{2-} ions on CO chemisorbed on cobalt atoms located at the periphery of the cobalt particles with the formation of $Co(CO)_4^-$ and CO_3^{2-} species. On the Co/SiO_2 system only the IR manifestations of CO linearly adsorbed on cobalt particles are detected.

ACKNOWLEDGMENTS

This research was carried out with the financial support of the Ministero Publica Istruzione, Progetti di Rilevante Interesse Nazionale. One of us (K.M.R.) thanks the "Third World Academy of Sciences," ICTP, Trieste, Italy, for awarding a grant for him to participate in this research.

REFERENCES

1. Huizinga, T., and Prins, R., *J. Phys. Chem.* **87,** 173 (1987).
2. Zecchina, A., Scarano, D., Marchese, L., Coluccia, S., and Giamello, E., *Surf. Sci.* **194,** 531 (1988).
3. He, J. W., and Moller, P. J., *Surf. Sci.* **180,** 411 (1987).
4. Mohana Rao, K., Spoto, G., Guglielminotti, E., and Zecchina, A., *J. Chem. Soc. Faraday Trans. 1* **84**(6), 2195 (1988).
5. Schneider, R. L., Howe, R. F., and Watters, K. L., *Inorg. Chem.* **23,** 4593 (1984).
6. Borello, E., Zecchina, A., Morterra, C., and Ghiotti, G., *J. Phys. Chem.* **71,** 2495 (1967).
7. Sheppard, N., and Nguyen, T. T. (Eds.), "Advances in Infrared and Raman Spectroscopy" (R. J. H. Clarke and R. E. Hester, Eds.), Chap. 2, p. 67. Heyden, London, 1978.
8. Sato, K., Inoue, Y., Kojima, I., Miyajaki, E., and Yasumori, I., *J. Chem. Soc. Faraday Trans. 1* **80,** 841 (1984).
9. Hollins, P., and Pritchard, J., *in* "Vibrational Spectroscopy of Adsorbates" (R. F. Willis, Ed.), Chemical Physics Series 15, p. 125. Springer-Verlag, Berlin, 1980.
10. Edgelle, W. F., Yong, M. T., and Koizumi, N., *J. Amer. Chem. Soc.* **87,** 2563 (1965).
11. Zecchina, A., Spoto, G., Garrone, E., and Bossi, A., *J. Phys. Chem.* **88,** 2586 (1984).
12. Braterman, P. S., "Metal Carbonyl Spectra," Academic Press, London/San Diego, 1975; and references therein.
13. McVicker, G. B., *Inorg. Chem.* **14,** 2087 (1975).
14. Zecchina, A., Platero, E. E., and Arean, C. O., *Inorg. Chem.* **27,** 102 (1988).
15. Mohana Rao, K., Spoto, G., Guglielminotti, E., and Zecchina, A., *Inorg. Chem.*, in press.
16. Chini, P., and Albano, V., *J. Organometal. Chem.* **15,** 433 (1968).
17. Chini, P., *J. Chem. Soc. Chem. Commun.*, 440 (1967).
18. Chini, P., Albano, V., and Martinengo, S., *J. Organometal. Chem.* **16,** 471 (1969).
19. Morterra, C., Zecchina, A., Coluccia, S., and Chiorino, A., *J. Chem. Soc. Faraday Trans. 1* **73,** 1544 (1977).
20. Palmer, D. A., and Van Eldic, R., *Chem. Rev.* **83,** 651 (1983).
21. Nakamoto, K., "Infrared Spectra of Inorganic and Coordination Compounds," p. 169. Wiley, New York 1963.
22. Wender, I., and Pino, P., "Organic Synthesis via Metal Carbonyls," Vol. I, p. 63. Wiley, New York, 1968.
23. Knözinger, H., "Proceedings of the 5th International Symposium on Relations between Homogeneous and Heterogeneous Catalysis, Novosibirsk, 1986" (Y. Yermakov and V. Likholobov, Eds.), p. 789. VNU Science Press, Utrecht, The Netherlands, 1987.